

Development of a Vibroimpact Device for the Resonance Hammer Drilling

Romulo R. Aguiar¹ and Hans I. Weber¹

¹ Mechanical Engineering Department, PUC-Rio
Rua Maquês de São Vicente, 229, Gávea
22453-900, Rio de Janeiro - RJ - Brazil
romulo@mec.puc-rio.br
hans@mec.puc-rio.br

*Abstract: Hard rock drilling is still a great challenge for oil companies. One current line of research involves combining the two existing drilling techniques in order to enhance the rate of penetration. This new technique is called **Resonance Hammer Drilling**. This article proposes the design and development of the first prototype that will operate in resonance, and will be capable of generating considerable dynamic forces. This device will be known as the **Resonant Impact Device**, or “RIMD”. In principle the idea is to build some sort of a “black box”, which will be mounted on a vibrating structure with two switches – one calibrating the RIMD resonance frequency and the other acting on the impacts – changing the size of the gap. It is known from previous work that gap size also has influence on the system natural frequency. Therefore there is a relationship between switches. One of the first steps of RIMD design and development is device dimensioning, necessary in order to construct a scale model at the Dynamic and Vibration laboratory at PUC-Rio representative of the real size system. The real size system will be mounted on the drillstring. RIMD components involve a mass-spring system with low damping and some impact and a gap variation device. The analysis of this prototype includes obtaining key characteristics such as the range of possible frequencies and the measurement of the generated impulsive forces. Finally, the built prototype will be used to validate an analytical model that will allow further investigations on this subject providing the way to other possible constructions.*

Keywords: nonlinear dynamics, vibroimpact systems

NOMENCLATURE

n = number of rollers in a roller cone bit

F_i = contact force, N

k_i = contact stiffness, N/m

c_i = viscous damping, Ns2/m

n_i = nonlinear factor

m_1 = drillstring mass, kg

k_1 = drillstring stiffness, N/m

c_1 = drillstring damping, Ns2/m

m_2 = RIMD mass, kg

k_2 = RIMD stiffness, N/m

c_2 = RIMD damping, Ns2/m

F_0 = excitation force amplitude, N

Greek Symbols

δ = impact penetration, m

$\dot{\delta}$ = penetration velocity, m/s2

Ω = excitation force frequency, rad/s

INTRODUCTION

A new drilling technique called **resonance hammer drilling (RHD)** has been studied by PUC-Rio University and CSIRO-Petroleum (Franca, 2004) (Detournay, 2004), as an alternative to increase the rate of penetration (ROP) in hard rocks drilling, Fig. 1(a).

This technique has as premise to use the already existent vibrations in the drillstring, in fact the axial vibration due to the cutting process, to generate a harmonic load on the bit and an excitation in a steel mass (hammer). When this excitation frequency is near to the steel mass natural frequency and, since the steel mass displacement is limited in positive direction by the gap, impacts on the bit occur. Therefore, besides the rotative penetration, where the teeth of the bit penetrate in the rock when the drillstring rotates, a percussive penetration happens due to the impact of the hammer with the bit, increasing the rate of penetration (ROP), although the impulsive force generated by the hammer should never be larger than the preload (weight on bit, or WOB), due to the possibility of the bit bounce effect (Franca, 2004), causing drillstring failure. Moreover, the hammer resonance frequency should not coincide with any drillstring natural frequency. Actually, when the exciting frequency, which is equal to the frequency of the bit displacement (due to the bit rolling over the lobed bottom hole) corresponds to an axial natural frequency of the drillstring, then resonance occurs and the drillstring can bounce. Consequently, one way to minimize the response to vibrations is to avoid drillstring rotations that induce natural frequency vibrations.

A first investigation of RHD is presented by Franca in 2004 (Franca, 2004). In this work, a model for the longitudinal

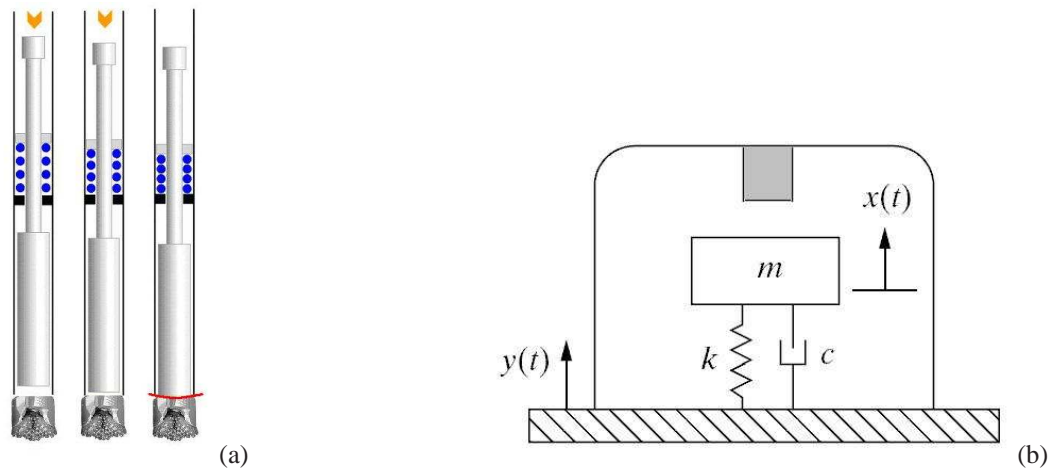


Figure 1 – a) Resonance hammer drilling technique.; b) Vibroimpact system.

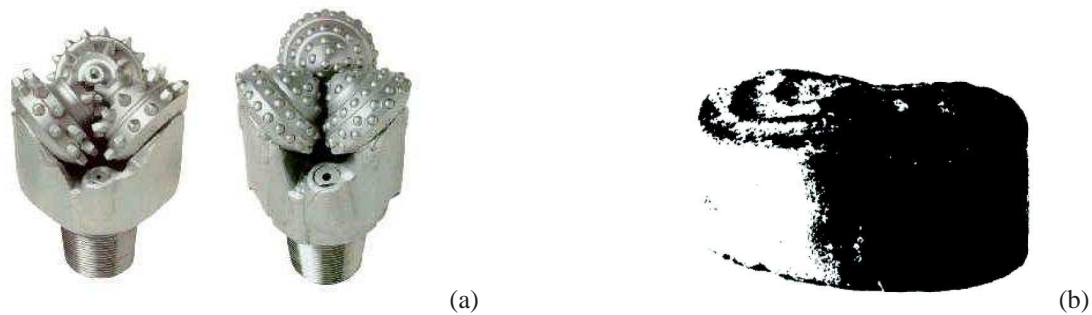


Figure 2 – a) Roller cone bits; b) lobe formation on the bottom hole, caused by the cutting process with roller cone bit.

behavior of the bit-rock with a vibroimpact system is investigated. As conclusion, the behavior of period-1 with one impact per cycle was always the best condition of penetration, increasing the ROP.

A second investigation is presented by Aguiar (Aguiar, 2006). In this work, a new mechanism to enhance the ROP is investigated. It is presented a test rig simulating the RIMD performance and the drillstring behavior influence on the RIMD. A numerical modeling (Aguiar and Weber, 2005) with experimental validation is also studied in order to predict the impact forces.

Objectives

A point that is still open about the resonance drilling technique is how to generate the dynamical load. All the idea in the investigations that were previously performed is that it is possible to obtain this load with the help of the rotary motion and the axial dynamics of the drillstring. To work out a first prototype that synthesizes all this ideas, this first development will address following points: it is needed an impact mass, that shall have very low damping on its motion in order to generate considerable amplitudes, which will be reduced through a gap and cause the impacts. The essential idea of the RIMD is observed in Fig 1(b).

There remain, however, a few questions that need to be addressed, such as: what kind of mass/motion is more adequate considering the space limitations to get a portable device? How to reduce damping? What are the possibilities to change the resonance frequency and in which range is this possible?

This means that in a first step there will be tested different possibilities using a shaker, displacement sensor and force gauge. After this selection there will be created an analytical model that describes the phenomena, which will be validated with help of experimental measurements. This model will allow an extrapolation to guess the obtained dynamic force through the action of resonance and impacts in the case of real sized systems.

The device concept shall be reduced to a device to be mounted on a structure; it shall have its properties validated and the action on a structure investigated. The construction of this prototype includes obtaining its characteristics, like the range of possible frequencies and the measurement of the generated impulsive forces. Once this concept is proven to work, it will be proposed the development of a vibro-impact device that shall operate in a resonant condition and be able to generate impulsive forces (RIMD).

The first idea following the previous work described above is to build a black box (RIMD) which, when mounted on a vibrating structure has two switches, one to calibrate a frequency in which the RIMD resonates and a second which acts on the impacts. It is known from former investigations that the size of the gap will change the resonant frequency. In this way there is dependence between the actions of both switches. The RIMD is included in a dynamic system to produce a vibroimpact process where the hammer periodically collides with the bit. The components of the RIMD are a moving mass, spring, very low damping and the way to produce and change the gap. Further possible parts are some active influence on the vibration and a control system to coordinate the actions.

The test rig mounted on the dynamics and vibration laboratory at PUC-Rio englobes a two-degree-of-freedom system with harmonic excitation, damping and impacts acting against a rigid support.

MATHEMATICAL MODELING

For the RIMD analysis, it will be necessary to incorporate the influence of the bit-rock interaction and the drillstring axial vibration behavior. For the bit-rock interaction, it is known that roller-cone bits, during the cutting process, generate an axial smooth movement of the drillstring with a frequency that is n times the rotary speed, where n represents the number of rollers (Dykstra, 1996). In most cases, $n = 3$. In this first approach, the bit-rock interaction and the drillstring axial vibration will be modeled as single degree-of-freedom system excited by an harmonic force. The system stiffness is associated to the drill pipes, which are responsible for transmitting the torque from the rotative table to the bit. The equivalent mass is directly associated to the drill collars (called also bottom hole assembly or simply BHA), responsible to provide weight on the bit (WOB). Main sources of damping in drillstrings are: viscous losses with the drilling mud, bit/rock interaction and friction with the hole walls. This should be enough to represent the influence of the drillstring on the RIMD.

The first RIMD prototype may be modeled as a single degree-of-freedom system which is coupled to the drillstring (more precisely, the actual RIMD concept is to attach the device inside the drillstring). The stiffness is provided by steel beam springs and the damping factor is associated to small friction losses and material damping.

For the impact force, the contact model used here is proposed by Hunt and Crossley (Hunt and Crossley, 1968), which consists of a nonlinear spring in parallel with a nonlinear damping. The contact force, F_i , is established by the following equation:

$$F_i(\delta, \dot{\delta}) = -k_i \delta^{n_i} - c_i \delta^{n_i} \dot{\delta} = -k_i \delta^{n_i} (1 + \lambda_i \dot{\delta}) \text{ with } \lambda_i = \frac{c_i}{k_i} \quad (1)$$

Where δ is the penetration, $\dot{\delta}$ the penetration velocity, k_i the contact stiffness and c_i some viscous damping. The factor n_i depends on the geometry characteristics of the contact surface. An important aspect of this model is that damping depends on the penetration. This is physically sound since contact area increases with deformation and a plastic region is more likely to develop for larger penetrations. Another advantage is that the contact force has no discontinuities at initial contact and separation, but it begins and finishes with the correct value of zero. This model has been studied and used by several authors and experimentally the model with a non-linear damping term represents quite well the real behavior of the system during impact (Gilardi and Shaft, 2002).

The entire model to be studied, a 2 degree-of-freedom mass-spring system with damping and impact (Aguiar and Weber, 2005), is shown in Fig. 3.

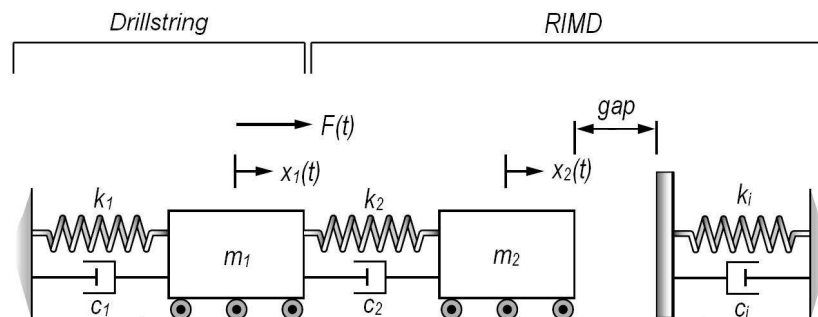


Figure 3 – System modeling.

That leads into two sets of equations: one for the case where m_2 is not in contact (2) and another set of equations for the contact situation (3):

$$\begin{cases} \dot{x}_1 = \frac{1}{m_1} [-(c_1 + c_2)\dot{x}_1 - (k_1 + k_2)x_1 + F_0 \sin(\Omega t) + c_2\dot{x}_2 + k_2x_2] \\ \dot{x}_2 = \frac{1}{m_2} [-c_2\dot{x}_2 - k_2x_2 + c_2\dot{x}_1 + k_2x_1] \end{cases} \quad (2)$$

$$\begin{cases} \dot{x}_1 = \frac{1}{m_1} [-(c_1 + c_2)\dot{x}_1 - (k_1 + k_2)x_1 + F_0 \sin(\Omega t) + c_2\dot{x}_2 + k_2x_2] \\ \dot{x}_2 = \frac{1}{m_2} [-c_2\dot{x}_2 - k_2x_2 + c_2\dot{x}_1 + k_2x_1 - k_i(x_2 - gap)^{n_i} (1 + \lambda_i\dot{x}_2)] \end{cases} \quad (3)$$

which becomes a nonlinear dynamic problem due to the discontinuity and impact. All simulations were solved using a 5th order Runge-Kutta method. Once the tolerances used during the simulations were extremely tight ($10^{-7} = 0.00001\%$ accuracy), no interpolation was used to determine the point of contact, since this tolerance is narrow enough to produce satisfactory results.

EXPERIMENTAL RESULTS

Test rig apparatus, methodology and parameter identification

The experimental apparatus attempts to represent the drillstring axial behavior and its influence over the impact device (RIMD), according to the simplifications previously discussed. The experimental apparatus is show on Fig. (4) and Fig. (5) .



Figure 4 – Test rig photo.

The experiment is composed by two separate systems, both moving from the equilibrium position over the vertical direction. The first system englobes the main support (steel) and the main cantilever beam (steel), with 370 mm of total length and a transverse section of 25 mm width and 5 mm height. A shaker is held to the main beam through a rigid coupling (screw) at 100 mm from the mounting.

The second system is composed by the RIMD, which is a mass-spring coupled to the main beam. The RIMD stiffness is assured by two clamped-clamped bending beams (steel) coupled to the first system by aluminum couplings. These beams has a transverse section of 22.3 mm width and 0.6 mm height. Besides, the length of these beams can be changed in order to vary the RIMD stiffness. The RIMD mass is composed by one of the aluminum couplings and by the impact device (steel).

The experiment parameters are:

- the main beam stiffness, as the beam length is varied;
- RIMD stiffness, adjusted in the same way;
- and the impact device gap, a small mount that slides over a vertical groove machined on the secondary support, measured through a calibrated shim.

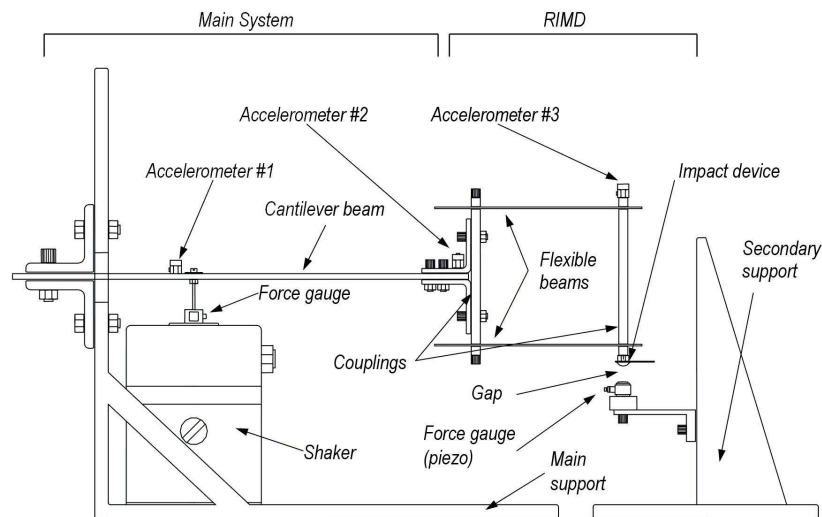


Figure 5 – Experiment scheme.

The input parameter is the force applied by the shaker (LDS V408 SN 457281) to the cantilevered beam. The shaker is operated by a signal generator (HP 35653C Source Module - part of signal analyzer HP 35650). The generator signal passes through a power amplifier (LDS PA100E) before get to the shaker.

The outputs are:

- the force applied by the shaker, obtained from a force gauge (Endevco 2311-100 SN 2348), mounted on the shaker;
- acceleration signals from accelerometers mounted is different points of the test rig, according to Fig. (5).
- the impact force applied by the RIMD over a piezo force gauge (Endevco 2311-100 SN 2472).

The methodology applied is to observe the behavior of the impact system as the RIMD stiffness is decreased and the gap is varied. There were chosen 4 different RIMD stiffness and 3 different gap sizes giving 12 possible combinations. For each stiffness/gap combination, firstly a brief study of the system without impact is carried out, aiming at identifying the test rig parameters for the established stiffness/gap combination. For that purpose, the natural frequencies are determined, as well as the values of stiffness and damping.

After that, a study with impact is carried out. The excitation frequency from the shaker is changed in order to sweep the range of the system natural frequencies. In this article it is shown the results from one RIMD stiffness and 3 different gaps.

For the masses, stiffness and damping, the parameter identification of the test rig follows the literature existing modal analysis and logarithmic decrement. For the impact coefficients (Hunt & Crossley impact model), a smaller experiment was performed, where a well known initial condition was imposed to the system and the experimental response was compared to the response of the equivalent mathematical model, where the impact model coefficients were adjusted.

For the experimental results shown here, all the parameters involved are shown on Tab. (1).

Experimental results

First, for the system without impact, the parameters are identified and the natural frequencies are obtained and compared with the mathematical model. These results are shown on Tab. (2). The study of the system without impact is considered in order to determine which range of frequencies will be swept, so all characteristics of the system with impact are observed.

Observing the system frequency response and the data shown on Tab. (2), it has been determined that the excitation frequency variation would be from 2.75Hz to 16Hz, in 0.25Hz increments. That variation is enough to capture all experiment phenomena.

System with impact, gap 0mm

By carefully observing all the experimental results, it has been concluded that the behavior of the system with impact may be divided into 5 different frequency bands. In the first excitation frequencies (from 2.75Hz to 4.75Hz), the impact

Table 1 – Test rig parameters.

Main beam			
mass	m_1	368×10^{-3}	kg
stiffness	k_1	2850	N/m
damping	c_1	1.269	Ns/m
RIMD			
mass	m_2	360×10^{-3}	kg
stiffness	k_2	272.1	N/m
damping	c_2	0.079	Ns/m
Impact parameters			
stiffness	k_i	$92.5 \cdot 10^3$	N/m
damping-stiffness ratio	λ_i	8	
nonlinear factor	n_i	0.9	

Table 2 – Natural frequencies - numerical/experiment comparison, system without impact.

Natural frequencies	Numerical	Experimental
First	4.1 Hz	3.9 Hz
Second	16.0 Hz	14.5 Hz

force presents a behavior of difficult characterization, since the system sometimes performs several impacts per cycle, sometimes two impacts per cycle and even one impact per cycle, with a low F_i/F_0 ratio. All these phenomena are presented below, on Fig. 6. Once in the same frequency band the observed phenomena is similar, most of the experimental data is omitted.

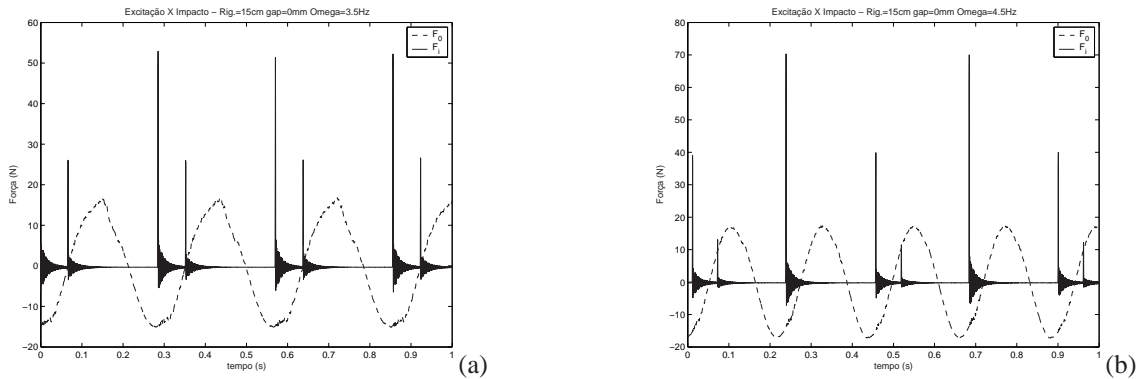


Figure 6 – Force response over time. RIMD stiffness 272.1N/m; gap 0mm. a) $\Omega = 3.25\text{Hz}$; b) $\Omega = 4.5\text{Hz}$.

On a second frequency band (from 5Hz to approximately 10 Hz), the impact characterizes as period-1 (1 impact per cycle), passing through the first system natural frequency with impact, in approximately 7.75 Hz. As the excitation frequency is varied, besides the variation of the force magnitude, the phase difference between the excitation force (F_0) and the impact force (F_i) varies too. These phenomena are presented on Fig. 7 and Fig. ??.

Notice that it has been used a tool for linear analysis (resonance) on a nonlinear phenomena. In this paper it is understood as resonance the point where the impact force ratio, F_i/F_0 (focus of this work), is maximum. The linear analysis tools and terminology will be used throughout the text with such purpose.

From the experimental results and the experience acquired with the test rig, it is also noted that on all frequency bands the only relevant acceleration variation is caused by impact. When there is no impact between the RIMD and the surface, the observed accelerations are very small. This can be noticed on Fig. 8.

On a third frequency band (from 10 Hz to 12.75 Hz), the system goes through a change of impact behavior, namely from period-1 to period-0.5 (1 impact every 2 cycles), a fact that can be observed on Fig. (9). Nevertheless, the impact forces developed on this frequency band are very low, being of the excitation force magnitude. Besides, on this transition, the system goes through a chaotic behavior in which it can be noted time intervals where there is no impact or there are various impacts in a single oscillatory period.

The second system resonance (13.25Hz) presents impacts in period-0.5 (1 impact every two cycles). This characteristic

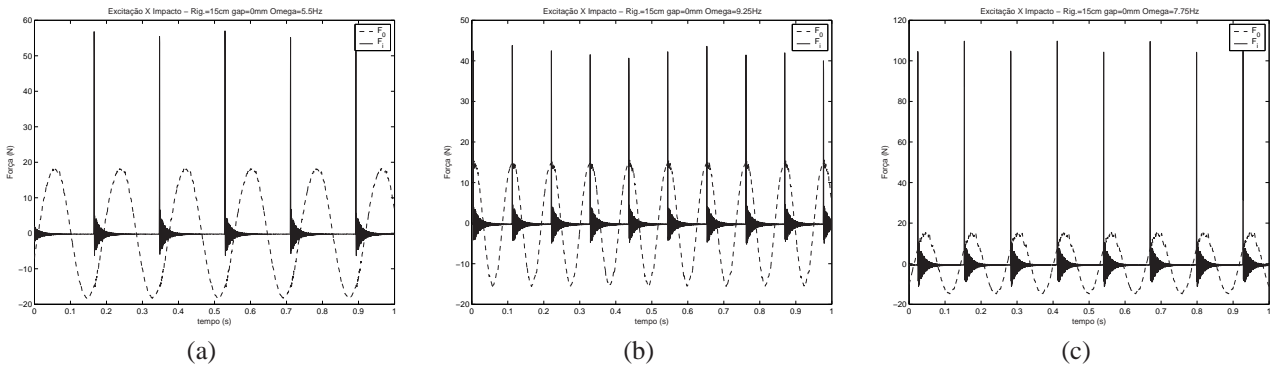


Figure 7 – Force response over time. RIMD stiffness 272.1N/m; gap 0mm. a) $\Omega = 5.5Hz$; b) $\Omega = 9.25Hz$; c) First resonance ($\Omega = 7.75Hz$).

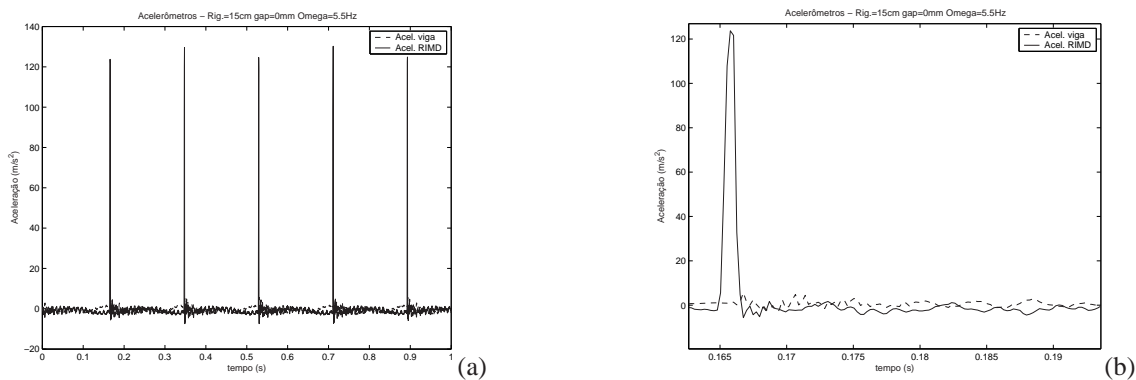


Figure 8 – Accelerations over time. Accelerometer #3 (solid line) and accelerometer # 2 (dashed line). a) $\Omega = 5.5Hz$; b) chart detail.

is observed on a frequency band from 12.75Hz to 16Hz.

For some stiffness/gap combinations, one final frequency band appears after the second system resonance. However, this frequency band shows a characteristic similar to the third band, where the impact force is low and some chaotic behavior appears.

With these data it is possible to analyze the system behavior in the frequency domain. For that, a computational routine is created so as to determine the F_i e F_0 values for each frequency studied. For the F_0 value, once the excitation force is cyclic, the amplitude value is adopted. For F_i , the maximum value is extracted. According to what was seen on Fig. 9, this routine to determine the impact force can mask the real results, since on certain frequency bands the impact force peaks do not reveal as constant and there are transitions in the behavior of the impact force. However, the purpose of this analysis is to obtain the optimal parameters that maximize the impact force and, according to what was seen in the experimental data analysis, the impact force reveals itself as periodic and constant on the frequency bands around resonance. Thus, despite the fact that the technique of obtaining only the maximum impact force values masks certain impact conditions (chaotic behavior), the analysis is valid as long as the main purpose is to determine the system optimal parameters which maximize the impact force and that, under these conditions, the F_i maximum force is constant. Finally, for making the chart non-dimensional so as to compare it to the answers in the other configurations, the force ratio F_i/F_0 . Thus, for these stiffness and gap conditions the force ratio chart (F_i/F_0) in the frequency domain is shown in the figure 11(a).

Some interesting facts can be observed from Fig. 11(a). It presents two peaks of maximum impact force in the studied frequency band, a fact that reinforces the hypothesis of using a 2 DOF model for modeling the experiment. The first resonance generates an impact force about 7.5 times bigger than the excitation force. The maximum force is obtained in the second resonance peak, where the F_i/F_0 ratio reaches 18. One final relevant fact is found on the frequency band near the first resonance, where the system presents a second force peak, around 6.75Hz, before the system reaches the maximum force.

Another interesting phenomenon to be noted here concerns the system natural frequencies without and with impact. For the first resonance, the presence of the impacts significantly altered the system natural frequency. This alteration of natural frequency due to the impacts presence was already studied (Mattos and Weber, 1997) and was expected, according to what was verified in the numerical study (Aguiar and Weber, 2005). Nevertheless, the same alteration is not verified for

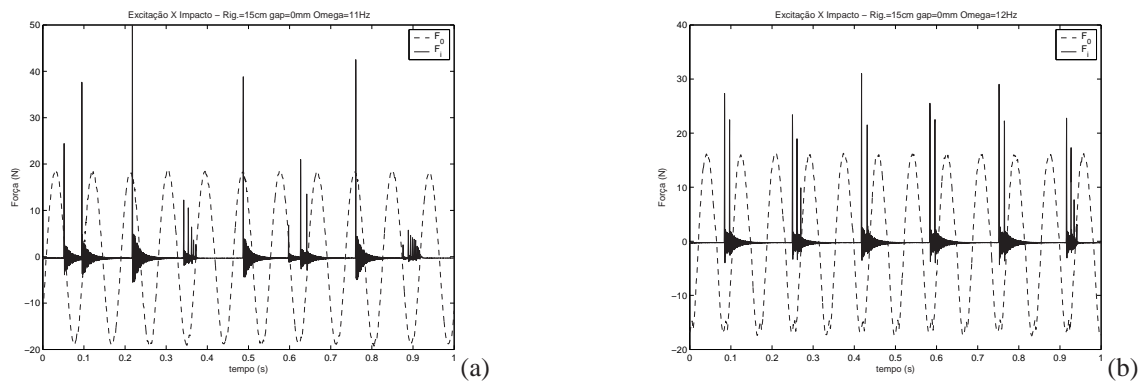


Figure 9 – Force response over time. RIMD stiffness 272.1N/m; gap 0mm. a) $\Omega = 11Hz$; b) $\Omega = 12Hz$.

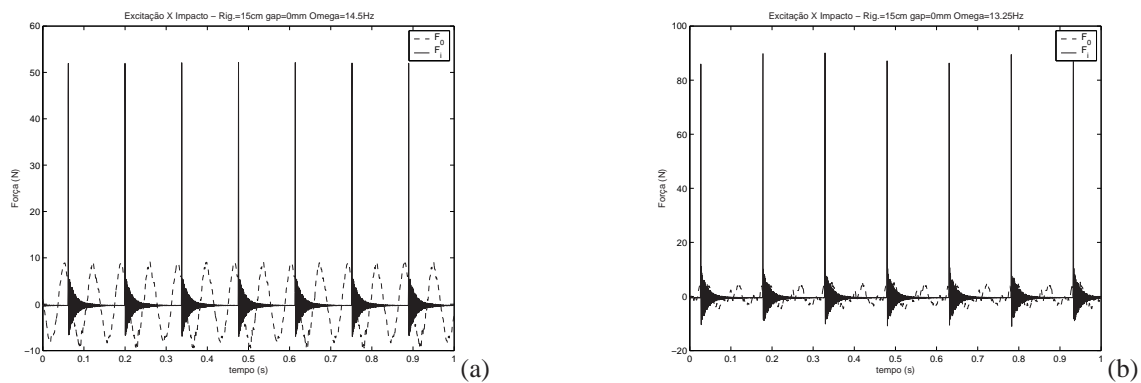


Figure 10 – Force response over time. RIMD stiffness 272.1N/m; gap 0mm. a) $\Omega = 13.25Hz$; b) $\Omega = 14.5Hz$.

the second frequency peak, and the 0.5Hz difference can be attributed to imprecision in the experimental determination of this frequency.

At this point it is important to note that the first natural frequency is directly related to the RIMD resonance, as the second natural is associated to the main beam. Notice that the concept of this drilling technique is to put the RIMD in resonance, not the main system. This means that although the maximum force ratio was found for the second resonance, the article focus will be on the first resonance.

From the experience acquired with the experiment, for a possible use on the field, it is recommended to work always with the system first natural frequency, for although it develops impulsive forces smaller than in the second frequency peak, the first resonance possesses more stability, that is, a variation of the excitation frequency around the natural frequency results in a small variation of impulsive force, which doesn't happen in the second resonance.

System with impact, gaps 1mm and 3mm

In a way similar to the 0mm system, the answer of the 1mm and 3mm gaps system can also be classified according to the frequency band imposed in the excitation.

For this experimental analysis, it is possible to compare the impact force for each chosen gap, keeping the RIMD stiffness constant. The chart is shown in Fig. 11(b).

In this analysis can be noticed a variation of natural frequency for the first resonance (natural frequency increases with gap decrease). In this frequency, the maximum value of the force ratio is found in the configuration of 3mm gap, whose ratio reaches the value of 12. For the second resonance, the gap variation does not seem to influence the natural frequency, since there is no significant alteration of that value with the gap change. For the three studied gaps the maximum value was found for 1mm gap, with a ratio of approximately 27.

MATHEMATICAL MODEL VALIDATION

This section aims at validating the numerical model shown in the previous section through numerical-experimental comparison. The test rig attempts to represent the drillstring axial behavior and its influence on the impact device (RIMD), according to the simplifications proposed before. The experimental analysis and parameters identification were carried out previously.

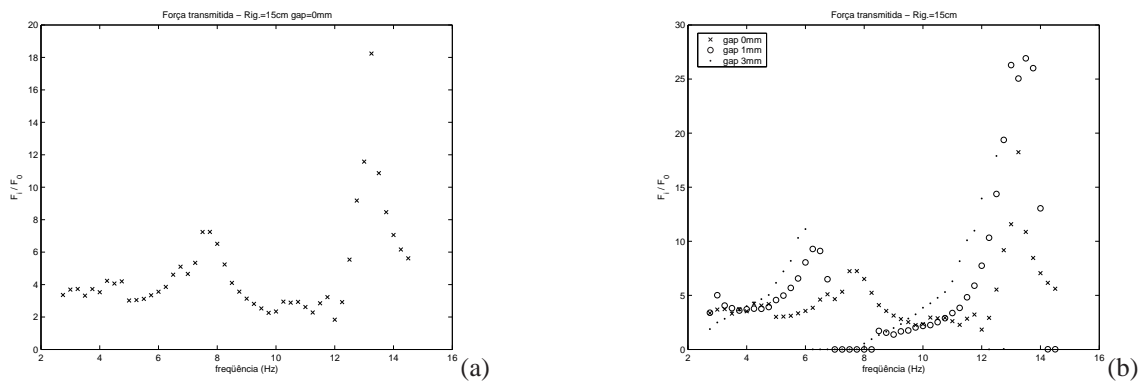


Figure 11 – Frequency domain response. RIMD stiffness 272.1N/m; F_i/F_0 versus Ω . a) gap 0mm; b) comparison between gaps.

Solving the equations (2) and (3) using the test rig parameters, the answers are obtained, in the frequency domain, of the impact force generated by the RIMD.

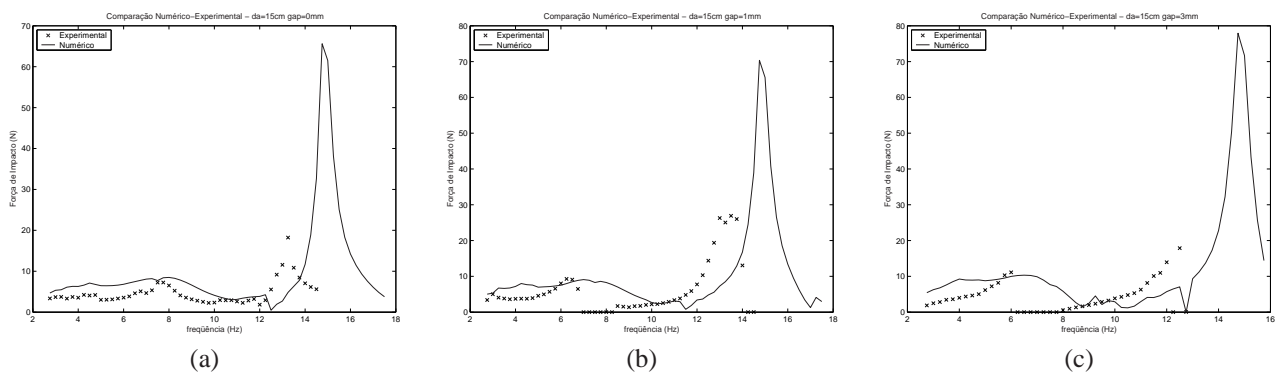


Figure 12 – Numerical-experiment comparison; RIMD stiffness 272.1N/m; F_i/F_0 versus Ω . a) gap 0mm; b) gap 1mm; c) gap 3mm.

From Fig. (12) it is verified that the numerical answer somehow follows the experimental data, although the numerical answer seems to be “dephased” from the experimental result, that is, the events (resonances, for example) in the numerical case occur in a higher frequency than in the real case. For the first resonance, the numerical model can reproduce satisfactorily the impact force maximum value. For the second resonance, however, the numerical results do not reproduce the experiment.

The frequency and impact force peak values, for the numerical case as well as for the experimental results, are compared on table (3). Another characteristic that the model does not reproduce is the non-linear jump of the impact force after the resonance, in the non-zero gap cases. For this situation, it is defined non-linear jump the sudden fall of the impact force in frequencies just above the natural frequency.

Table 3 – Natural frequencies and maximum impact forces; first resonance; numerical and experiment; RIMD stiffness 272.1N/m.

Natural frequencies	Experiment	Numerical
gap 0mm	7.75 Hz	8.0 Hz
gap 1mm	6.25 Hz	7.0 Hz
gap 3mm	6.00 Hz	6.5 Hz
Impact forces	Experiment	Numerical
gap 0mm	7.25 N	8.5 N
gap 1mm	9.3 N	9.2 N
gap 3mm	11.1 N	10.4 N

As mentioned, it is recommended always to work with the first system natural frequency, aiming at generating impulsive forces, since in spite of developing impact forces smaller than in the second resonance, the first natural frequency has

more stability. So, the numerical model, although presenting a strong simplification when considering a 2 DOF system, is satisfactory in the application scope in which we are interested.

CONCLUSIONS

This article presented the proposal and design of a new device to enhance the rate of penetration in hard rock drilling, called **resonance hammer drilling**. A test rig was designed and built in order to incorporate the RIMD and reproduce the drillstring axial vibration behavior.

On the experimental analysis, while studying the impact force characteristic, sweeping the excitation frequency, it was noted that, in all stiffness/ gap combinations, there was a certain standard of system behavior which could be divided in frequency bands. During the first system natural frequency, the impact was characterized of period-1 (1 impact per cycle). As the excitation frequency was varied, besides the variation of the impact force magnitude, the phase difference between the excitation force (F_0) and the impact force (F_i) also varied. For the first resonance there was practically no system influence on the *shaker*, a fact confirmed by the shape of the excitation curve F_0 in the time domain.

Finally the results of each configuration were compared so as to obtain the optimal impact condition. From the experience acquired with the experiment it was recommended to work always with the first system natural frequency, for field applications, for in spite of developing impulsive forces smaller than in the second frequency, due to system stability.

A mathematical model was validated using the experimental data. Although the model is not capable to describe all phenomena observed in the experimental analysis, the numerical answer somehow follows the experimental data. For the first resonance (focus of the study), the numerical model can reproduce satisfactorily the impact force maximum value and the resonance frequency.

ACKNOWLEDGMENTS

The authors wish to thank CNPq and FAPERJ for its support of this research.

REFERENCES

- Aguiar, R.R., 2006, "Desenvolvimento de um Dispositivo Gerador de Vibroimpacto", MSc Thesis, Department of Mechanical Engineering, PUC-Rio, Rio de Janeiro, Brazil.
- Aguiar, R.R. and Weber, H.I., 2005, "Optimum Parameters of a Vibroimpact Device", Proceedings of the XXVI CIL-AMCE, Guarapari, ES, Brazil.
- Detournay, E., 2004, "Enhanced Bit Performance through Controlled Drillstring Vibrations - Phase 3", Technical Report, Drilling Mechanics Group, CSIRO Petroleum, Bentley, WA, Australia.
- Dykstra, M.W., 1996, "Nonlinear Drillstring Dynamics", PhD Thesis, Department of Petroleum Engineering, University of Tulsa, Oklahoma, USA.
- Franca, L.F.P., 2004, "Perfuração Percussiva-Rotativa Auto-Excitada em Rochas Duras", PhD Thesis, Department of Mechanical Engineering, PUC-Rio, Rio de Janeiro, Brazil.
- Gilardi, G. and Sharf, I., 2002, "Literature survey of contact dynamics modeling", Mechanism and Machine Theory.
- Hunt, K.H. and Crossley, F.R.E., June 1968, "Coefficient of Restitution Interpreted as Damping in Vibroimpact", Journal of Applied Mechanics - Transactions of the ASME, pgs 440 to 445.
- Mattos, M.C. and Weber H.I., 1997, "Some Interesting Characteristics of a Simple Autonomous Impact System with Symmetric Clearance", ASME - Design Engineering Conference.

RESPONSIBILITY NOTICE

The author(s) is (are) the only responsible for the printed material included in this paper.